

Characteristics of the blast pressure by the difference in fracture situation in the reinforced concrete (RC) wall

Kana Nishino^{*†}, Shiro Kubota^{**}, Yuji Wada^{**}, Yuji Ogata^{**}, Norio Ito^{***},
Masayuki Nagano^{***}, Satoki Nakamura^{***}, and Mieko Kumasaki^{*}

^{*}Yokohama National University, 79-7 Tokiwadai, Hodogaya-ku, Yokohama-shi, Kanagawa, 240-8501 JAPAN
Phone: +81-45-339-3994

[†]Corresponding author: nishino-kana-wr@ynu.jp

^{**}Research Institute of Science for Safety and Sustainability (RISS), National Institute of Advanced Industrial Science and Technology, 16-1 Onogawa, Tsukuba-shi, Ibaraki, 305-8569 JAPAN

^{***}Sagami Kogyo Co., Ltd., 1-3-12 Yoshinodai, Chuo-ku, Sagamihara-shi, Kanagawa, 252-0222 JAPAN

^{****}Kayaku Japan Co., Ltd., KFC Bldg. 9F, 1-6-1 Yokoami, Sumida-ku, Tokyo, 130-0015 JAPAN

Received: June 25, 2017 Accepted: October 30, 2017

Abstract

This study focuses on the blast pressure characteristics of small-scale blasting in rescue work. It was found that the peak overpressure at the borehole side was larger than that at the back side in the single-charge experiments. The peak overpressure for a Type A fracture, which created a crater only at the borehole side, was larger than the peak overpressure of a Type B fracture. Since a Type B fracture generates craters on both sides of the wall, it was expected that more energy would be expended in fracturing the wall than in Type A. However, the peak overpressure at the back side in our experiments was nearly the same in Type A and B fractures.

The effectiveness of a blasting sheet in reducing peak overpressure at the borehole side was evaluated in model disaster scene experiments. The blasting sheet decreased peak overpressure by approximately 80% compared to when no blasting sheet was used, for the largest peak overpressure, occurring at a scaled distance of $3.5 \text{ m} \cdot \text{kg}^{-1/3}$. We set a safety standard for overpressure in small-scale blasting, based on the results of previous studies. We observed that peak overpressure was much lower than this safety standard when the blasting sheet was used.

Keywords: blast pressure, small-scale blasting, fracture type, borehole side, blasting sheet

1. Introduction

Breaching (by small-scale blasting) for rescue work has the potential to impact the surroundings due to explosion. The small-scale blasting generates a blast wave, flying debris and noise, which can collapse the vulnerable structure and affect the human body. Accordingly, it is important to evaluate the impacts to prevent a secondary disaster. Among all the adverse effects, the blast wave can have the most severe consequences. For example, a blast wave can deal a fatal blow to a weakened building and strike the human body, causing direct or indirect

consequences. A direct consequence is an injury caused by the impact of the blast wave, while an indirect consequence is injury due to falling or collision, after a body is blown away by the blast wave¹⁾.

For safety standards, the blast wave is fundamental in determining the distance between a residence and a magazine in Japan²⁾. The result obtained from a free-air explosion experiment conducted by Baker³⁾ and a surface burst experiment using TNT conducted by MITI⁸⁷⁴⁾ were used to establish the current safety standards. Apart from establishing standards, the importance of understanding

blast pressure attracts researchers to study air blast effects as a function of the moisture content of the soil⁵⁾, the relation between the blast wave and explosive loading density^{6), 7)} etc. In these reports, the blast pressure was assumed to be generated by several kilograms of explosive.

The present safety standard may not be applicable to small-scale blasting used in rescue work. Small-scale blasting uses several grams of explosive per hole, and the total of amount of explosive weights around 100 g. Studies of blast pressure caused by small-scale blasting are generally lacking.

In this study, therefore, blast pressure, particularly its relation to fracture type, was investigated through single-charge experiments. The model disaster scene experiments used reinforced concrete (RC) wall prepared as a sample. Based on the experimental results, the safety of charge conditions applicable to small-scale blasting for rescue work was evaluated.

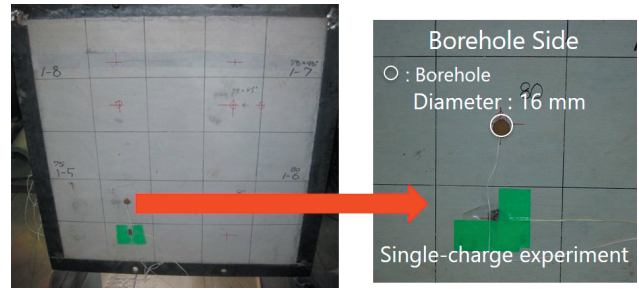
2. Model experiments

2.1 RC wall sample and charge conditions

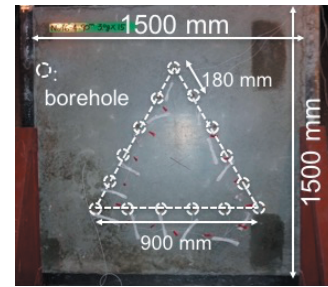
A sample of the RC wall is shown in Figure 1. The thickness of the RC walls was 150, 180, 200, 230, and 250 mm. The width and height of 150 mm thick RC wall were 1500 mm. The width and height of other walls was 1200 mm. The diameter of the reinforcing bars was 13 mm. For the 150 mm RC wall, the bars were placed in a grid pattern in the middle of the wall. For the other walls, the bars were placed in a grid pattern at 50 mm from each surface of the wall. The concrete density was 2300 kg·m⁻³. The average compressive strength of concrete was 27.7 MPa for the 150 mm thick RC wall or 27.1 MPa for the other walls after 28 days.

The experiments to obtain primary blast wave data were conducted on 150 mm thick RC wall with single-charge of 3.0 g of explosive each, using borehole depths of 75, 80, 85, and 90 mm⁸⁾. Figure 1 (a) shows the setting for the single-charge experiments. Boreholes were drilled vertically into the wall. The borehole diameter was 16 mm, and clay was used as a stemming material.

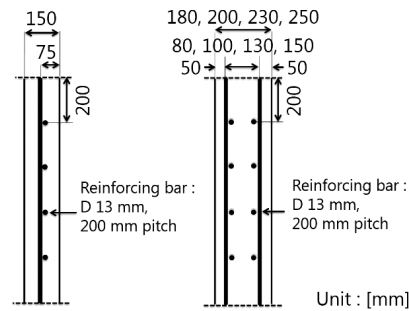
Model disaster scene experiments were conducted using the RC walls with 150, 180, 200, 230, and 250 mm of thickness. Figure 1 (b) shows the setting for the model disaster scene experiments. The boreholes were spaced in triangular shape, and the distance between holes was fixed at 180 mm. The explosives in the boreholes were



(a) Single-charge experiment



(b) Model disaster scene experiment, 150 mm thick RC wall



(c) Cross-sectional view

Figure 1 Sample of the reinforced concrete (RC) wall.

detonated at the same time. The charge condition for those experiments is shown in Table 1. A blasting sheet (TS-12K, SBKOGYO Co., Ltd.) was used to control the blast wave.

2.2 Measurements

A blast pressure sensor, 137A23 (PCB Piezotronics Inc.) was employed to measure the blast wave. Timing of this measurement was controlled by accurate blasting machine, which has 0.1 μs accuracy. In the single-charge experiments, the blast pressure sensors were placed 1.0 m from the surface of both borehole side and back side. The position of the blast pressure sensors is as shown in Figure

Table 1 Charge conditions for the model disaster scene experiments.

Thickness of the RC wall [mm]	Borehole depth [mm]	Amount of explosive per hole [g]	Total of amount of explosive [g]	A number of boreholes	Fracture type ⁸⁾ [Type A or B]
150	75	3.0	45	15	Type A
150	90	3.0	45	15	Type B
180	95	4.0	60	15	Type A
180	117, 126	6.0, 5.0	85	15	Type B
200	110	5.0	75	15	Type A
230	120	6.0, 7.0	97	15	Type A
250	131	7.0	42	6	Type A

2 and Table 2. For the model disaster scene experiments, the distance of the blast pressure sensor was changed according to the planned fracture type. The direct impact of the blast wave on a human body was investigated by assuming that no obstacle was present between the

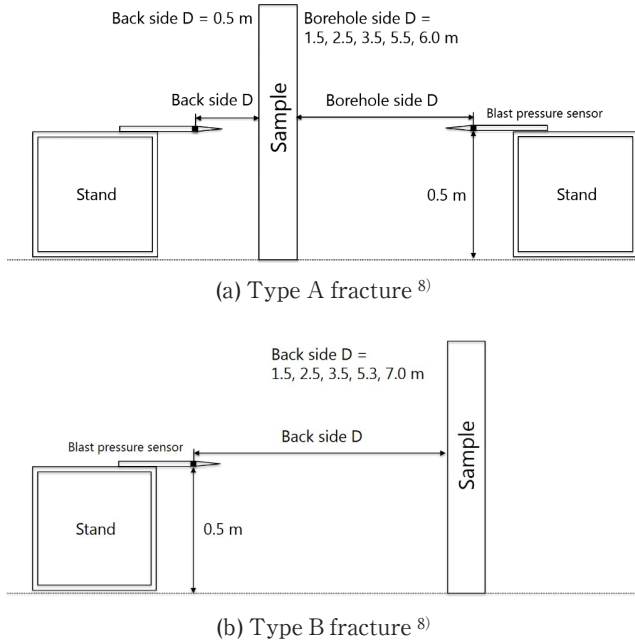


Figure 2 Schematic diagram of the experimental setup of the blast pressure sensor.

Table 2 The positions of the blast pressure sensor for the model disaster scene experiments.

Thickness of the RC wall [mm]	Fracture type ⁸⁾ [Type A or B]	Distance from the borehole side surface [m]	Distance from the back side surface [m]
150	Type A	2.5, 3.5	0.5
150	Type B	–	2.5, 3.5, 5.3, 7.0
180	Type A	1.5, 5.5	0.5
180	Type B	–	1.5
200	Type A	1.5, 5.5	0.5
230	Type A	1.5, 6.0	0.5
250	Type A	1.5, 5.5	0.5

explosion center and the person.

For data analysis, the Hopkinson-Cranz scaled distance⁹⁾, which is calculated using Equation (1), was used to compare results without taking the amount of explosive and the distance of the blast pressure sensor from the RC wall into consideration.

$$Z = R / \sqrt[3]{W} \tag{1}$$

where Z is the scaled distance [$\text{m} \cdot \text{kg}^{-1/3}$], R is the distance from a sample to a blast pressure sensor [m], and W is the amount of explosive [kg].

3. Results and discussion

3.1 Single-charge experiments

3.1.1 Fracture type observed in single-charge experiments with the 150 mm thick RC wall

The experimental results with single-charge are shown in Table 3. In our previous study⁸⁾, two fracture types were confirmed. Type A fractures generated a crater on the borehole side and cracks on the back side. Type B fractures created craters on both sides. Type B fractures created larger craters on the back side than on the borehole side.

3.1.2 Relationship between the blast wave and time

Figure 3 shows the blast pressure-time profile observed 1.0m away from the RC wall sample. The black line indicates Type A fractures, and the red line indicates Type B fractures.

As shown in Figure 3 (a), a typical pressure-time profiles

Table 3 Experimental results with the single-charge condition.

Borehole depth [mm]	Fracture type ⁸⁾ [Type A or B]	Crater volume (borehole side) [$\times 10^3 \text{ mm}^3$]	Crater volume (back side) [$\times 10^3 \text{ mm}^3$]
75	Type A	330	cracks
80	Type A	128	cracks
85	Type B	110	2204
90	Type B	117	1852

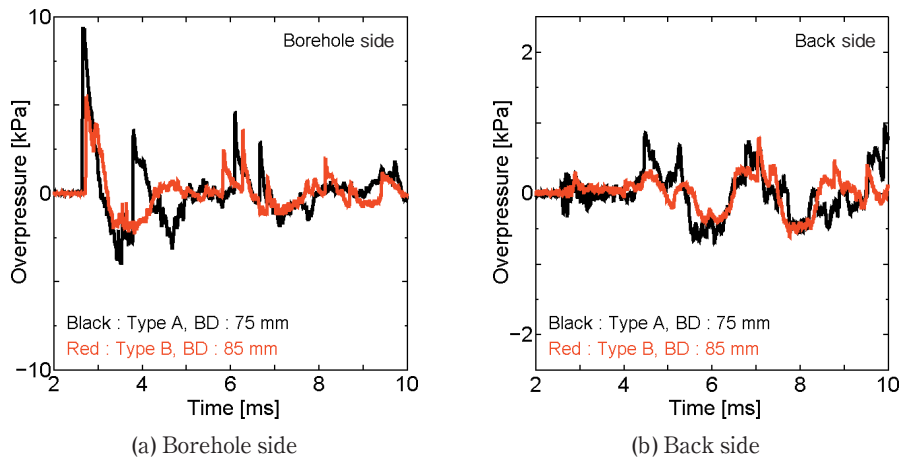


Figure 3 Typical examples of pressure - time profile. Single-charge experiments, 150 mm thick RC wall, 3.0 g of explosive
 Black: Type A fracture, Borehole depth: 75 mm
 Red: Type B fracture, Borehole depth: 85 mm
 BD: Borehole depth

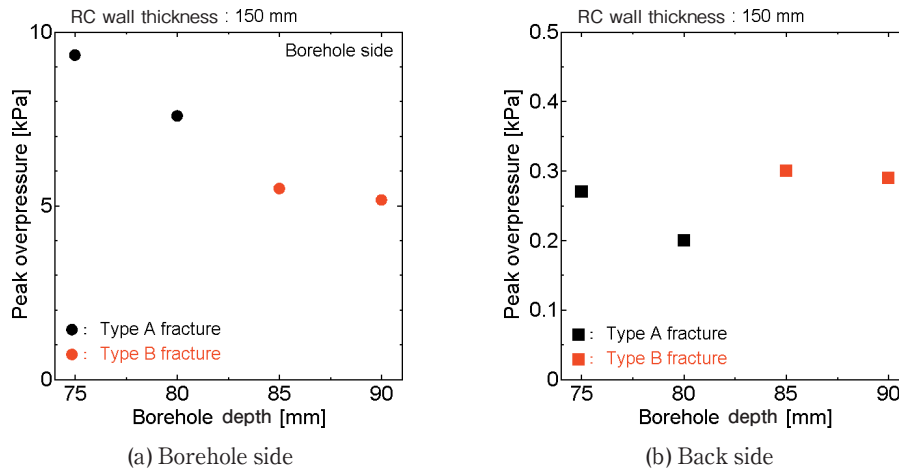


Figure 4 Relationship between the peak overpressure and the borehole depth.

at the borehole side of Type A and B fractures were similar to the profile obtained in a free space explosion conducted without the presence of a wall^{10,11}. That is, the blast pressure profile reached a peak overpressure, and then decreased rapidly. The peak overpressure was recorded at 2.7 ms after the explosive detonated. The positive pressure continued for approximately 0.4 ms. Subsequently, the blast pressure decreased.

At the back side, as shown in Figure 3 (b), the peak overpressure was observed at 2.7 ms in both Type A and B fractures. An overpressure of 1 kPa was recorded at 4.5 and 7.0 ms in Type A fractures. The increase of the blast pressure on the borehole side can be explained by the fact that the experiments were conducted in an enclosed space. The blast wave leaked from the borehole and propagated into the air. Subsequently, it reflected off the wall in the experimental space. The blast wave might have come around to the back side of the wall, and the diffracted blast wave might have built up blast pressure on the back side. The interaction of a blast wave with a column was studied by Shi et al¹². When the blast wave strikes the column, the blast wave is partially reflected by the surface of column and partially diffracted around it. In this process, the diffracted blast wave may interact with the wave directly generated into the back side, thereby increasing the amplitude. Some researchers have conducted experiments and numerical simulations of blast wave interaction with small components^{13–17}. The second and third peak overpressure might be due to the interaction between blast waves occurring at the borehole side and back side, which might be a problem in a rescue work. However, this phenomenon would be unlikely to occur at rescue site because RC walls have two free surfaces, which means that the blast wave leaked from the borehole cannot reach the back side. Therefore, hereinafter, this study focused on the first peak overpressure which is shown in Figure 3.

3.1.3 Relationship between blast wave and borehole depth

The relationship between the first peak overpressure and the borehole depth is shown in Figure 4. As is shown in Figure 4 (a), the peak overpressure decreased as the borehole depth increased for Type A fractures, which

created a crater only at borehole side. The experiments with borehole depth of 85 mm and 90 mm exhibited almost the same peak overpressure for Type B fractures. Since Type B fractures generated craters on both sides of the wall, they consumed more fracture energy in the wall than Type A fractures. The explosion energy is consumed in the deformation and fragmentation of the concrete wall, and the rest of the energy is transformed into blast wave, vibration, and noise¹⁸. This explains why the peak overpressures observed in Type B fractures were smaller than ones in Type A fractures; in Type A, the peak overpressure energy was not consumed in crater generation.

However, the peak overpressure at the back side was less than 0.4 kPa, regardless of the fracture situation. In case of Type A fractures, the explosion gas leaked from the borehole side⁸, since the cracks were only created by the shock wave. In Type B fractures, a crater was also generated on back side. Thus, the explosion gas leak from the back side lagged, and some of its energy was used to scatter debris⁸. For both Type A and Type B fractures, the peak overpressure on the back side was the shock wave that reached the back side of the wall and interfered with the air.

In summary, the blast pressure of the borehole side was greater than that of the back side in the small-scale blasting tests, regardless of the fracture situation.

3.2 Validity assessment of the blasting sheet as protective measure

3.2.1 Model disaster scene experiments

The single-charge experiments indicated that the peak overpressure at the borehole side was larger than at the back side. This phenomenon is significant for Type A fractures, which are applicable to rescue situations where victims are present at the back side. Therefore, overpressure reduction at the borehole side is essential.

The effectiveness of a blasting sheet was evaluated as a means to address this problem. The blasting sheet is light and can be folded, enabling rescue crew to carry it easily. Crews are expected to ensure the safety of both the victims and themselves with the sheet, by covering the borehole side before ignition, to confine debris and reduce

Table 4 Data on the injury effects of explosion: Direct blast effects²⁰.

Effective peak overpressure [kPa]	Effect
34.5	Eardrum rupture
82.7	Lung damage

overpressure. In this study, a polyester blasting sheet was selected from among other available material such as rubber. The weight of the chosen blasting sheet was approximately 12 kg. The width and height of this blasting sheet were 4000 and 6000 mm, and the thickness was 0.7 mm. The blasting sheet is shown installed on the borehole side in Figure 5 (a), and Figure 5 (b) depicts the situation after blasting, showing that the blasting sheet was able to limit the dispersion of debris.

3.2.2 The effect of the blasting sheet

The peak overpressure as a function of the scaled distance is shown in Figure 6. In this study, the air burst of 3.0, 6.0, and 9.0 g of C4 explosive were measured as a basis peak pressure. For comparison, measurements of surface bursts of C4 explosive¹⁹ obtained in a previous study are plotted on this figure as well. The experiments without the blasting sheet showed that the peak overpressure corresponded with the basis peak pressure. However, peak overpressure decreased to approximately 79% of that observed with the surface bursts of C4 explosive, even at $3.2 \text{ m} \cdot \text{kg}^{-1/3}$, where the largest peak overpressure was observed in this study. Therefore, it was confirmed that the peak overpressure of small-scale blasting was less than the peak overpressure of the surface burst, even when the blasting sheet was not used.

Moreover, the peak overpressure with the blasting sheet was 4.9 kPa, an approximately 80% reduction from that without the blasting sheet at $3.5 \text{ m} \cdot \text{kg}^{-1/3}$, where the largest peak overpressure was observed in the experiments. Further, the peak overpressure measured at the back side was smaller than that measured at the borehole side, regardless of whether a blasting sheet was used or not.

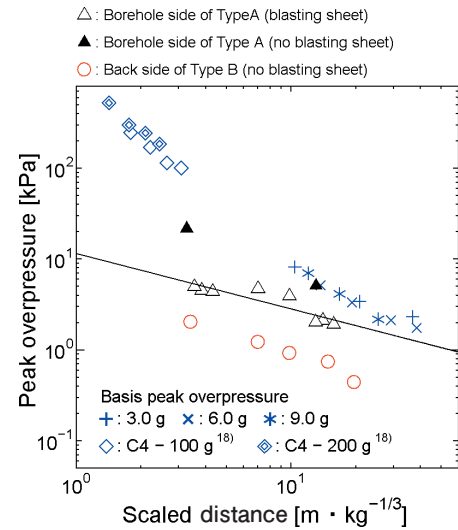
The typical peak overpressure causing injuries is



(a) Set of the blasting sheet



(b) Reduced the fragmentation

Figure 5 Proposal of protective measures using a blasting sheet.**Figure 6** Relationship between the scaled distance and peak overpressure.

summarized in Table 4²⁰. These data imply that these effects appear when blast pressure is applied to the human body for 3 milliseconds. Previous research²¹ showed that people can be blown away by the blast wave and injured, and that injury can be incurred at 15.9 kPa of blast pressure. More than 6.2 kPa of overpressure leads to temporary hearing loss. Therefore, we set the safety standard of overpressure for small-scale blasting at 6.2 kPa to ensure harmless overpressure for the human body. When the blasting sheet was applied, the overpressure was much smaller than this safety standard, ensuring the safety of those involved in the rescue.

4. Conclusion

Small-scale blasting for rescue work has the potential to impact the surroundings due to explosion. Because it uses a new blasting charge technique, there have been few studies that can be applied to developing a safety standard for this method. This study conducted single-charge experiments to obtain data to establish these safety standards. The experiments evaluated the relation between fracture type and blast pressure, and showed that the peak overpressure at the borehole side was greater than that at the back side.

In addition to the single-charge experiments, experiments intended to reproduce a disaster scene were carried out. In these experiments, the blasting sheet was used to reduce the peak overpressure at the borehole side. The results showed that the influence of the blast wave on the surrounding environment was reduced to a peak overpressure lower than the safety standard defined in this study. This study showed that the appropriate charge condition, with a proper safety measure such as a blasting sheet, can ensure the safety of people and surroundings when small-scale blasting is used for rescue work in a closed environment.

Acknowledgment

This study was supported by the Promotion Program for Scientific Fire and Disaster Prevention Technologies in 2012 and 2013.

References

- 1) T. Ohno, K. Fujimoto, K. Iida, K. Fujikake, M. Beppu, and Y. Someya, "Kisokarano Bakuhatu anzen kougaku", Morikita Publishing Co., Ltd., 38–40 (2011).
- 2) M. Yoshida and Y. Nakayama, *EXPLOSION*, 17, 2–5 (2007). (in Japanese).
- 3) W. B. Baker, "Explosions in Air", Univ. Texas Press (1973).
- 4) Y. Nakayama, M. Yoshida, Y. Kakudate, M. Iida, N. Ishikawa, K. Kato, H. Sasaki, S. Usuba, K. Aoki, N. Kuwabara, K. Tanaka, K. Tanaka, and S. Fujiwara, *Kogyo Kayaku (Sci. Tech. Energetic Materials)*, 50, 88–92 (1989). (in Japanese).
- 5) Y. Nakayama, D. Kim, K. Ishikawa, K. Wakabayashi, T. Matsumura, and M. Iida, *Sci. Tech. Energetic Materials*, 69, 123–128 (2008).
- 6) H. Ichino, T. Ohno, K. Hasue, and S. Date, *Sci. Tech. Energetic Materials*, 70, 38–42 (2009). (in Japanese).
- 7) H. Ichino, T. Ohno, K. Hasue, and S. Date, *Sci. Tech. Energetic Materials*, 71, 51–57 (2010). (in Japanese).
- 8) K. Nishino, S. Kubota, Y. Wada, Y. Ogata, N. Ito, M. Nagano, A. Fukuda, and M. Kumasaki, *Sci. Tech. Energetic Materials*, 77, 40–46 (2016).
- 9) P. D. Smith and J. G. Hetherington, "Blast and Ballistic Loading of Structures", Elsevier Science Ltd. 37–41 (1994).
- 10) P. D. Smith and J. G. Hetherington, "Blast and Ballistic Loading of Structures", Elsevier Science Ltd. 35 (1994).
- 11) Y. Uehara and T. Ogawa, "Technical Handbook for Fire and Explosion Protection", *TECHNO SYSTEM* 397–400 (2004).
- 12) Y. Shi, H. Hao, and Z. X. Li, *Shock Waves*, 17, 113–133 (2007).
- 13) D. Kh. Ofengeim and D. Drikakis, *Shock Waves*, 7, 305–317 (1997).
- 14) J. Le, *Communications in Nonlinear Science & Numerical Simulation*, 4, 1–7 (1999).
- 15) S. Ohyagi, T. Obara, F. Nakata, and S. Hoshi, *Shock Waves*, 10, 185–190 (2000).
- 16) G. O. Thomas and R. Ll. Williams, *Shock Waves*, 11, 481–492 (2002).
- 17) C. Wu and H. Hao, *International Journal of Impact Engineering*, 31, 699–717, (2005).
- 18) K. Hashidume, *Architectural product-engineering*, 281, 58–61 (1989). (in Japanese).
- 19) K. Ohkubo, H. Ohyama, M. Beppu, T. Ohno, and M. Katayama, *Journal of Structural Engineering. A*, 53A, 1273–1283, (2007). (in Japanese).
- 20) S. Mannan, "Less's Loss Prevention in the Process Industries Hazard Identification, Assessment and Control Volume2", Butterworth-Heinemann, 1590–1592 (2012).
- 21) U. S. Army, *Structures to Resist the Effects of Accidental Explosions*, TM5–1300 (1990).